Neutron-removal cross sections of ^{6,8}He, ^{8}Li and ^{9,10}Be nuclei

B.M. Hue [1,2], T. Isataev [2], S.M. Lukyanov [2], K. Mendibaev [2,4],
A.G. Artukh [2], D. Aznabayev [2], C. Borcea [2], P.V. Cuong [1],
B. Erdemchimeg [2], S.A. Klygin [2], G.A. Kononenko [2],
K.A. Kuterbekov [4], V.A. Maslov [2], V.Ostashko [5],
Yu.E. Penionzhkevich [2,6], F. Rotaru [3], Yu. Sereda [2],
A.N. Vorontsov [2], T.D. Thiep [1]

[1]*Institute of Physics, Hanoi, Vietnam*
[2]*Flerov Laboratory of Nuclear Reactions, Dubna, Russian Federation*
[3]*National Inst. for Physics and Nuclear Engineering, IFIN − HH, Bucharest Magurele, Romania*
[4]*L.N. Gumilyov Eurasian National University, Astana, Kazakhstan*
[5]*Nuclear Physics Institute, Kyev, Ukraine*
[6]*National Research Nuclear University "MEPhI", Moscow, Russian Federation*

Neutron-removal cross-section (σ_{-xn}) measurements of neutron-rich light nuclei were performed on the COMBAS fragment-separator with a multi-detector Si telescope at intermediate energies (22-34) MeV/nucleon. The removals of one neutron from ^{8}Li and ^{9}Be, two neutrons from ^{6}He and ^{10}Be and four neutrons from ^{8}He were observed from the reactions on a Si-CsI(Tl) telescope. Results of σ_{-xn} for ^{6}He, ^{8}He, ^{8}Li, ^{9}Be and ^{10}Be nuclei were obtained and compared with those of previously measured data. The data indicate that ^{4}He is a good core within ^{6}He and ^{8}He. Furthermore, we found that ^{9,10}Be nuclei disintegrated by one- and two-neutron removal reaction, respectively.

Keywords: neutron-rich light nuclei, neutron-removal cross-section.

Introduction

The radioactive ion beam (RIB) technology was developed dramatically since 80s [1]. The progress with RIB allows studying nuclear reactions by exotic projectiles and discovering new regions of nuclear matter in extreme states mentioned in [2]. In particular, it has become possible to determine the nuclear size and matter distribution for unstable nuclei, mainly based on the interaction and reaction cross sections. Interaction cross-section (σ_I) measurements, which were the first experiments using RIBs at high-energy (800 MeV/nucleon), started at the Bevalac of the Lawrence Berkeley Laboratory (LBL) in the early 80s [3]. Soon after, measurements of reaction cross-section (σ_R) started at GANIL [4]. There are two major methods to measure σ_R at intermediate energies. One is the associated γ-ray detection method [4] and the other is the transmission method using $B\rho \times \Delta E \times TOF$ or $\Delta E \times E$ identifications [5,6]. Utilizing neutron-rich and proton-rich light radioactive projectiles impinging on a reaction target such as the CsI(Tl) detector [7] or the Si detector to measure σ_R and nucleon-removal cross section for several weakly bound nuclei at bombarding energies near 50

MeV/nucleon [8,9] were performed many years ago. These data provide the information on projectile structure and matter distribution, including halo effect as well as indicating the relative strengths of different reaction modes. Additionally, measuring σ_{-xn} can provide more information about the wave function of the valence nucleon in halo-like nuclei [10] and display information with regard to the structure by a measurement of the total breakup yield [11]. Nevertheless, the data about σ_R and σ_{-xn} measured at various energies (20-800 MeV/nucleon) and on different targets is far from seeing complete.

In this experiment, we attempted to measure the σ_{-xn} for a number of light isotopes in the intermediate energy range. The experiment used the secondary beams of the stable and short-lived light nuclei produced by bombardment of a ^{22}Ne primary beam on a Be production target and subsequently separated and purified by the achromatic magnetic system of the COMBAS. The description of this separator is presented in [12]. A multi-detector Si and CsI(Tl), which is similar to that in [7,9], was used both as target and detection system. The obtained results of the σ_{-xn} measurement for weakly bound ^{6}He, ^{8}He, ^{8}Li, ^{9}Be and ^{10}Be nuclei in the energy range (22-34) MeV/nucleon are presented and compared to other experimental results.

The experimental set-up

The study of nuclear reactions induced by secondary beams requires magnetic separation and particle identification (PID) for fragments of interest. In our experiment, a primary ^{22}Ne beam was accelerated to around 35 MeV/nucleon of which intensity was up to 1 pμA by the U-400M cyclotron of the Flerov Laboratory of Nuclear Reactions, JINR and sent to a ^{9}Be target of 89 mg/cm^2 thickness. A secondary beam cocktail consisting of particles ^{6}He, ^{8}Li, ^{9}Be and ^{10}Be was produced and transported by the COMBAS fragment-separator system (Figure 1).
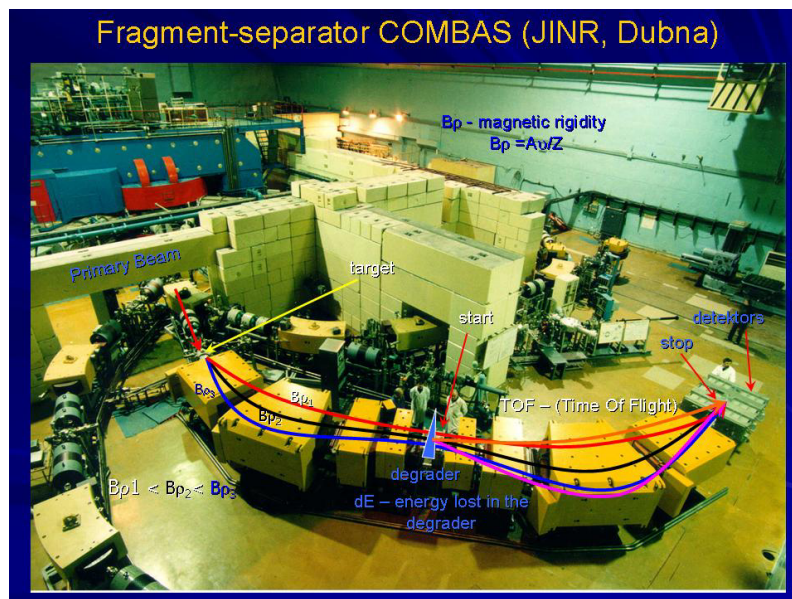

Figure 1. Experimental scheme of the COMBAS fragment separator.

The secondary beams were partially purified by 200 μm Al wedge. The energy dispersion was limited to less than 1 % FWHM by analyzing slits. At the fo-

cal point of COMBAS fragment separator, the secondary products were detected by a telescope consisting of four Si-detectors (ΔE) and E-detector CsI(Tl). This telescope served as the target, degrader of beam energy and detecting system for reaction. Figure 2 shows a schematic view of the telescope (not to scale). A first Si detector ΔE_1 (300 μm thick, 50 x 50 mm^2) was set into a cylinder chamber to obtain the ΔE information. Behind ΔE_1, there was a rectangular parallelepiped box containing ΔE_0 (500 μm thick, 50 x 50 mm^2) and two other detectors with 16 horizontal X strips and 16 vertical Y strips in rear side of ΔE_2 (300 μm thick, 55 x 55 mm^2) and ΔE_3 (300 μm thick, 55 x 55 mm^2), respectively. These detectors were designed for both measuring spectra of the secondary beams and determining the X-Y coordinate distribution. The silicon ΔE_4 (500 μm thick, 50 x 50 mm^2) detector was also installed inside the box to acquire the additional ΔE information and identification for heavy fragments that did not reach the detector behind. In order to measure the remaining energy of particles (E_r) a CsI(Tl) detector with 15mm thickness was used and mounted at the end of the telescope.
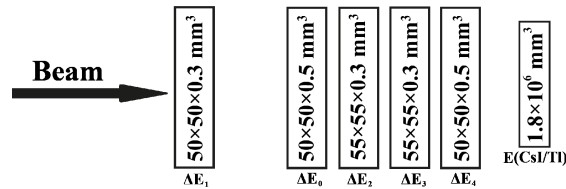

Figure 2. The telescope (not to scale) used in this experiment.

The used telescope allowed us to get the unambiguous particle identification by the $\Delta E \times E$ method. Expected energy losses in each detector were found by applying the Bethe-Bloch formula ($\Delta E/\mathrm{dx}$) $= Z^2 f(\nu)$. Total energy (E_{total}) was calculated as a sum of energy losses and remaining energy: $E_{total} = \sum \Delta E_i + E_r$.

Data analysis

The incident beam produced through fragmentation reaction and in-flight separation is generally a cocktail of isotopes. The goal of this section was to determine the total number of the incident beam of interest and estimate the contaminants. The principle of particle identification, as well as the selection, was described in the previous section. To investigate the incident beams, a combination of all available information from detectors was used, including the one by one of the detectors in front of the CsI crystal. The longest range isotopes were identified based on the information of energy loss in the ΔE_4 and the residual E_r in the CsI(Tl) detector. The thickness of CsI(Tl) detector was sufficient to stop all of the reaction products. Figure 3 shows the yields versus ΔE_2 and the total energy E_{total} of the incident isotopes measured during the experimental run for the secondary beam. These isotopes include both stable nuclei and neutron-rich nuclei.

For further data analyses, a gate around the isotope of interest (^{10}Be as an example) as a secondary beam was selected by an area cut from the double dimensional plots of energy losses in the first two detectors. To inspect the contaminants contributing to that secondary beam, we used energy spectrum from ΔE_4 and CsI(Tl) detector as in Figure 4. Various reaction channels were identified as shown by the labels (the areas inside of curves in Figure 4) from 1 to 6. These reaction channels consist of:
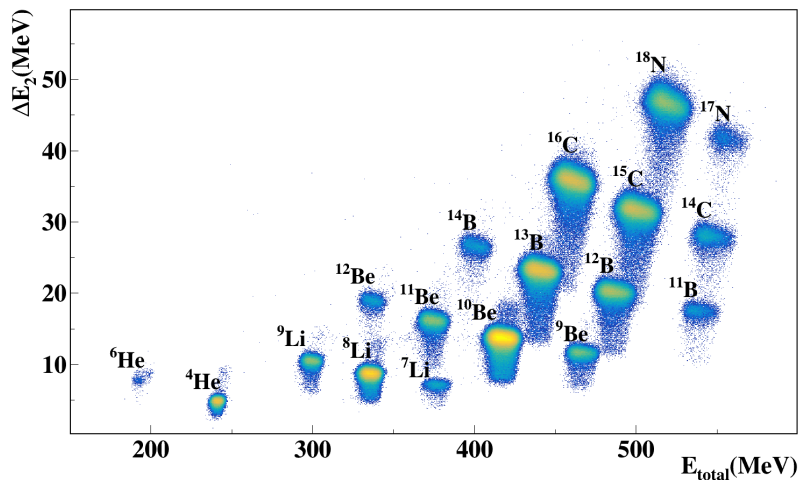
Figure 3. ETwo-dimensional energy spectrum of ΔE_2 (Si detector 300 μm) and total energy E_{total} .

- Zone 1: unreacted events,

- Zone 2: elastically and inelastically scattered events without changing atomic number,

- Zone 3: reacted events in the CsI(Tl) detector,

- Zone 4: out-of-acceptance events, which were not detected in the CsI(Tl) detector,

- Zone 5: channeling effect,

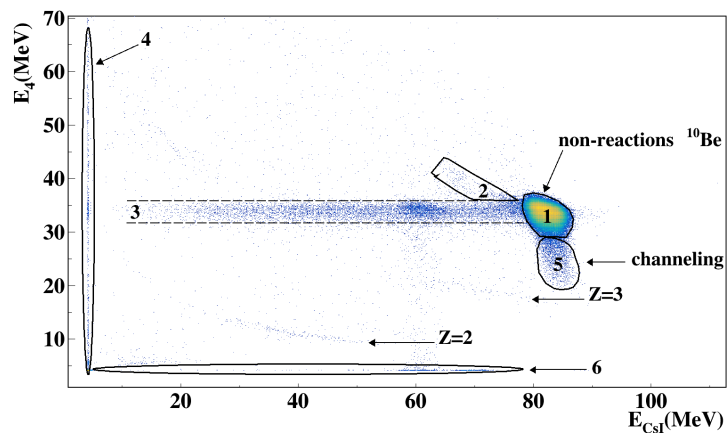- Zone 6: events stopped in CsI(Tl) detector but somehow ΔE_4 could not detect them.

Figure 4. Two-dimensional energy spectrum from detectors ΔE_4 and CsI(Tl) selected for 33 MeV/nucleon [10] Be incident upon the Si+CsI telescope shown in Figure 2.

Neutron-removal reactions, which produced fragments with the same proton number as the projectile but neutron number was less than that of the projectile,

were detected mostly in the stopping detector CsI(Tl) and its predecessor. Therefore, we only concerned about the unreacted events and reacted events in CsI(Tl) detector presented in the zone 1 and zone 3, respectively. The events in other zones were eliminated by combining small cut areas on all detectors placed in front of CsI(Tl) detector. One example is shown in Figure 5 for ^{10}Be.
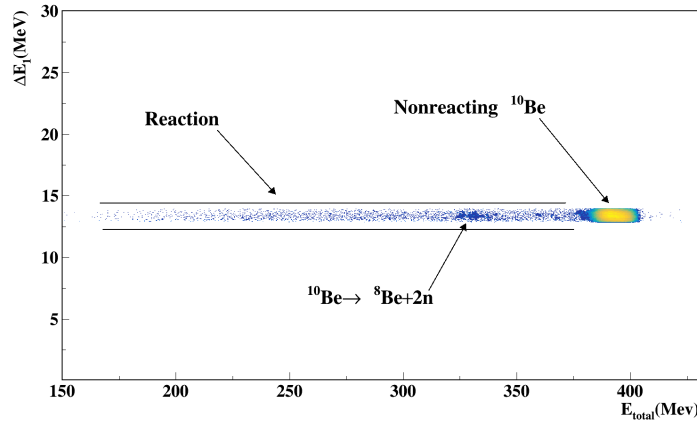

Figure 5. Purified two-dimensional energy spectrum of the combined cut of ^{10}Be in ΔE- E$_{total}$.

Charged fragments from neutron-removal reactions passed through several detectors before their ionization losses were distinguishable from others of non-reacting projectiles. To recognize what neutron-removal reaction happened, it was necessary to identify isotopes which appeared in the reacted area created in the band 3(Figure 5). Both the neutron-removal area and the non-reacting area have the same velocity and charge. Therefore, the mass number of the neutron-removal area can be determined as below:

$$A_{nr} = A_{non} * \frac{E_{nr}}{E_{non}} \tag{1}$$

where E_{nr}, E_{non}, A_{nr} and A_{non} are the energy of neutron-removal isotopes, the energy of non-reacting isotopes, the mass number of neutron-removal isotopes and the mass number of non-reacting isotopes, respectively.

Results and discussion

Yields in the one- and two-neutron removal peaks for ^{6}He, ^{8}Li, ^{9}Be and ^{10}Be were obtained by fitting a gaussian function as illustrated in Figure 6. After subtraction of other counts under neutron-removal peak, we calculated the cross section of neutron-removal reactions for nuclei of interest. The results have been given and compared with similar reported data in Table 1.

As the results, we obtained the projectile energy-deposition spectra presented in Figure 6, where counts versus total energy deposited in the telescope are shown for ^{6}He (halo nucleus), ^{8}Li, ^{9}Be and ^{10}Be. The energy distribution allows us to clarify the nuclear reaction mechanism. The off-scale peaks were produced by the non-reacting projectiles. The integral under these peaks were used to calculate the flux of the corresponding beams after the reaction target. The satellite peaks, which were produced by the neutron-removal reactions of ^{6}He,
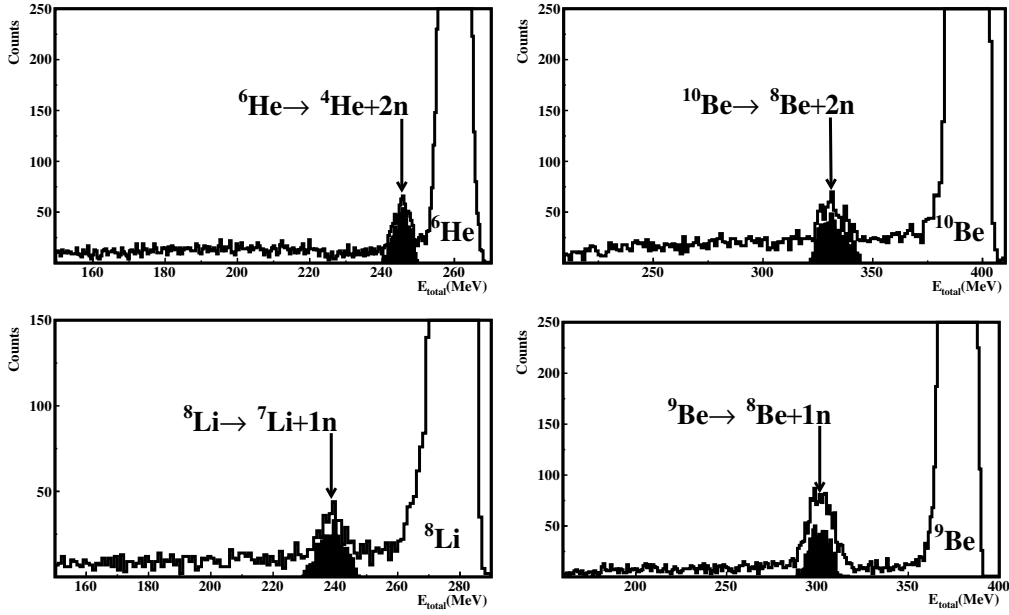
Figure 6. Energy-deposition spectra of ^{6}He, ^{8}Li, ^{9}Be and ^{10}Be projectiles in the telescope, with structures due to $2n$-removal from ^{6}He, ^{10}Be and 1n removal from ^{8}Li and ^{9}Be indicated.

^{8}Li, ^{9}Be and ^{10}Be nuclei with the telescope material, are very visible. Prominent groups for 1n and 2n removal were observed for ^{8}Li, ^{9}Be and ^{6}He, ^{10}Be group, respectively (Figure 6).

For the two-neutron-halo ^{6}He nucleus, the nuclear core is tightly bound and two-neutron-removal is one of the strongest reaction channels [13]. On average, the two neutrons from the break-up reaction carry off two-sixth of the remaining kinetic energy. ^{6}He nucleus shows a prominent two-neutron-removal peak above the continuum caused by ^{4}He core reaction in this experiment.

Another energy spectrum of identified ^{7}Li from ^{8}Li dissociation is shown in Figure 6. ^{8}Li is of interest not only as neutron-rich nucleus but also in connection with its role in nuclear astrophysics. It can be divided into two parts like typical studies of the loosely bound system, namely a core (^{7}Li) and a valence neutron. As another option, ^{8}Li has a small separation energy of 2.032 MeV for the valence neutron and is a mirror nucleus of the famous nucleus ^{8}B. There are still arguments in proton-halo nucleus structure of ^{8}B [14]. Hence, ^{8}Li will be a compelling candidate for exploring the formation of the halo structure. The dominant two-component structure of the ^{8}Li nucleus in the form of the ^{7}Li core and a "skin" of one neutron has been confirmed by one-neutron removal reaction in our experiment.

In case of Be isotopes, even though ^{8}Be is unbound we determined ^{8}Be after one- and two-neutron removal from the breakup of ^{9}Be and ^{10}Be, respectively. Decreasing neutron-removal cross section from those of ^{9}Be and ^{10}Be can be explained by the internal structure of nuclei. ^{9}Be has a Borromean structure including ^{8}Be (= $\alpha + \alpha$) nucleus together with an additional neutron with the relatively small binding energy S_{1n} (^{9}Be) = 1.665 MeV. On the other hand, ^{10}Be nucleus is better bound (S_{2n} (^{10}Be) = 8.477 MeV) and the nucleus is stiff against a variation in the distance of the α clusters [15]. In the low-lying states, the surrounding neutrons are moving in the mean-field of two α. In other words, the

coexistence of α cluster core and mean-field-like valence neutrons is presented from both ^{9}Be and ^{10}Be nuclei. These phenomena arise from the decoupling of scales α-particle clustering is an important concept in nuclear physics for light nuclei.

Our results with regard to neutron-removal cross section for ^{9}Be and ^{10}Be have been compared with other experimental data as in Figure 7. There are the marked differences between our data and others may be due to the dissimilarity of the reaction target. In a little more detail, Si (Z = 14) detector was used as an active target [9,16] not resembling CsI(Tl) (Z > 53) detector in this experiment. It is known that σ_{-xn} strongly depends on the charge number of target, which demonstrated in [17]. The dependence of σ_{-xn} on the charge number of targets and projectiles will be investigated in our following experiment.
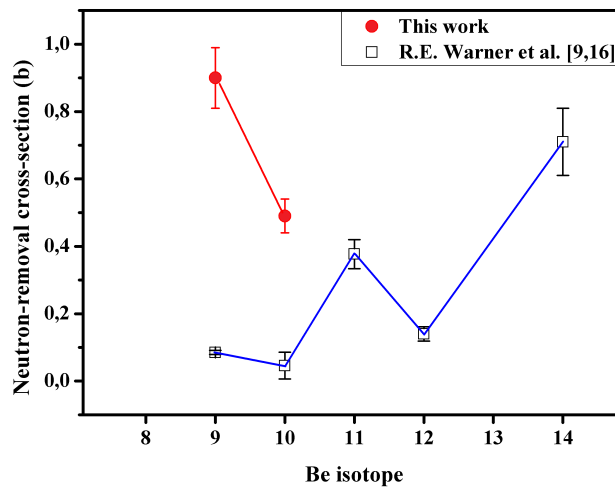

Figure 7. Experimental neutron removal cross-section of beryllium isotope from this work (red circle) compared with other result [16] (open square).

An intriguing situation we found for the case of ^{8}He at 22 MeV/nucleon energy. Occurred reaction of ^{8}He beam was predicted on account of 4n-removal. Nonetheless, the obtained n-removal cross section result is rather large $(1.82 \pm 0.7b)$ and large error bar is due to a low statistic (Figure 8).
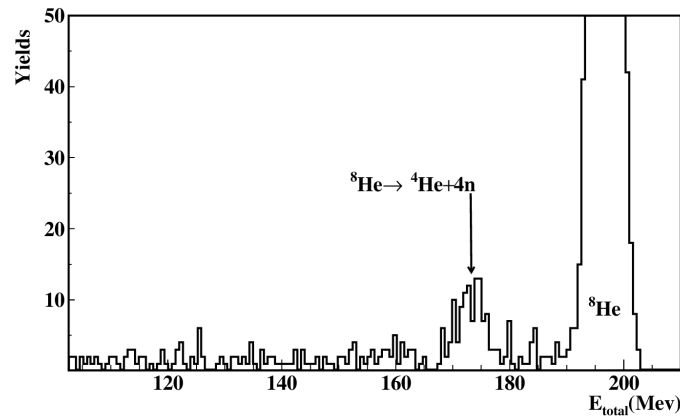

Figure 8. Energy-deposition spectrum of ^{8}He projectile in the telescope.

^{8}He, which is the heaviest bound He isotope has a matter radius similar to that of ^{6}He [5]. The binding energy is similar for both one neutron and

two neutrons of ^{8}He ($S_{1n}(^8$He$) = 2.534$ MeV, $S_{2n}(^8$He$) = 2.125$ MeV) and its four-neutron separation energy is $S_{4n}(^8$He$) = 3.1$ MeV whereas the 2n-removal processes in the ^{6}He are energetically favored with smaller binding energy ($S_{2n}(^6$He$) = 0.975$ MeV). The first experimental indication came from a compilation of cross-section data at 790 MeV/nucleon by I.Tanihata et al. [10] where the σ_I and two- and four- neutron removal cross sections in ^{4}He, ^{6}He and ^{8}He + C reactions were analyzed. They assumed a relationship between wave functions of the nuclear core and the valence nucleons in halo-like nuclei. By the experiment, they obtained the high-energy σ_I data containing an important information as the following relation is valid:

$$\sigma_I(^6He) - \sigma_{-2n}(^6He) \approx \sigma_I(^4He), \qquad (2)$$

$$\sigma_I(^8He) - \sigma_{-2n}(^8He) - \sigma_{-4n}(^8He) \approx \sigma_I(^4He). \qquad (3)$$

Also, in the framework of Glauber model, they found that ^{4}He persists as an unmodified core in ^{6}He or ^{8}He nucleus. In our experiment, we determined predominantly ($\alpha + 4n$) structure for ^{8}He. This suggests that ^{8}He may be described as an α-particle surrounded by four valence neutrons. Thereupon, we also confirmed by our study that ^{4}He is a good core for both ^{6}He and ^{8}He.

Table 1.
Measured neutron-removal cross sections from ^{6}He, ^{8}Li, ^{9}Be and ^{10}Be.

Nucleus	Energy (MeV/nucleon)	σ_{-xn} (b)	σ_R (b)	Source
^{6}He, σ_{-2n}	23.7	0.88 ± 0.09	-	this work
^{6}He, σ_{-2n}	29.0	0.47 ± 0.04	1.59 ± 0.06	[9]
^{8}Li, σ_{-1n}	29.4	0.59 ± 0.06	-	this work
^{8}Li, σ_{-1n}	25.3	-	1.58 ± 0.05	[9]
^{9}Be, σ_{-1n}	33.4	0.90 ± 0.09	-	this work
^{9}Be, σ_{-1n}	(48-63)	0.085 ± 0.006	1.63 ± 0.05	[16]
^{10}Be, σ_{-2n}	32.6	0.49 ± 0.05	-	this work
^{10}Be, σ_{-2n}	(46-60)	0.046 ± 0.004	1.54 ± 0.05	[16]

According to Table 1, at first glance it is clear that there are an anomalous small values of σ_{-1n} and σ_{-2n} for ^{9}Be and ^{10}Be resulted from [16]. Following those data σ_{-1n} for ^{9}Be and σ_{-2n} for ^{10}Be have approximately 5 % and 3 % of σ_R, respectively. This reflects a conflict in data [16] with the opinion that ^{9,10}Be are weakly bound nuclei and could be disintegrated mostly by neutron emission as naturally. As a consenquence, one might expect much large value of the neutron removal cross section, as we observed in our experiment.

There are systematic errors arisen in the data analysis including uncertainties in the fitting process to obtain the neutron-removal peak. In addition, other unpredictabilities such as event statistics, identification efficiency of the detectors, effective target thickness and beam attenuation have contributed the uncertainty of our results.

Conclusions

Secondary beams including a various isotope range from He to Be isotopes were produced and then separated by using the COMBAS fragment-separator.

The particle identification for secondary beam was performed by employing the ($\Delta E \times E$) method. The ΔE and E were measured by the Si and CsI(Tl) telescope, respectively. As the results, the neutron-removal cross sections of some neutron-rich light isotopes (^{6,8}He, ^{7,8}Li and $^{9-10}$Be) were obtained. The obtained data were compared with previous results [9,16]. We plan to carry out the next experiment on total reaction cross-section, neutron-removal cross section and elastic scattering measurements of other neutron-rich light nuclei using this technique and COMBAS fragment separator with improved statistics at various angles. The authors would like to thank for the support from the Russian Science Foundation (17-19-01170).

References

[1] I. Tanihata et al., Phys. Rev. Lett. **55**(1985) 2676.
[2] Yu. E. Penionzhkevich, Phys. At. Nucl. **77** (2014) 1400.
[3] I. Tanihata et al., Phys. Lett. B **160** (1985) 380.
[4] M.G. Saint-Laurent et al., Z. Phys. A **332** (1989) 457.
[5] Ozawa et al. Nucl. Phys. A **693** (2001) 32.
[6] F. Negoita et al., Phys. Rev. C **54** (1996) 1787.
[7] R. E. Warner et al., Phys. Rev. C **43** (1991) 1313.
[8] C. Borcea et al., Nucl. Phys. A **616** (1997) 231.
[9] R. E. Warner et al., Phys. Rev. C **54**, (1996) 1700.
[10] I. Tanihata et al., Phys. Rev. Lett. B **289** (1992) 261.
[11] D. Cortina-Gil et al., Eur. Phys. J., A **10** (2001) 49-56.
[12] A.G. Artukh et al., Nucl. Instrum. Methods. A. **426**, (1999) 605.
[13] T. Kobayashi et al., Phys. Lett. B **232** (1989) 51.
[14] Y.Y. Yang et al., Phys. Rev. C **87** (2013) 044613.
[15] M. Zakova et al., J. Phys. G **37** (2010) 055107.
[16] R. E. Warner et al., Phys. Rev. C **64** (2001) 044611.
[17] R. Anne et al., Phys. Lett. B **250** (1990) 19.